Published in final edited form as:

Cancer Res. 2018 January 01; 78(1): 246–255. doi:10.1158/0008-5472.CAN-17-1973.

Small molecule inhibition of Axl targets tumor immune suppression and enhances chemotherapy in pancreatic cancer

Kathleen F. Ludwig[1,2,†], **Wenting Du**[2,†], **Noah B. Sorrelle**[2], **Katarzyna Wnuk-Lipinska**[3], **Mary Topalovski**[2], **Jason E. Toombs**[2], **Victoria H. Cruz**[2], **Shinichi Yabuuchi**[4], **N.V. Rajeshkumar**[4,‡], **Anirban Maitra**[5], **James B. Lorens**[6], and **Rolf A. Brekken**[2,7,*]

[1]Division of Pediatric Oncology, Department of Pediatrics, University of Texas Southwestern Medical Center, Dallas, Texas, USA [2]Hamon Center for Therapeutic Oncology Research, Division of Surgical Oncology, Department of Surgery, University of Texas Southwestern Medical Center, Dallas, Texas, USA [3]BerGenBio AS, Bergen, Norway [4]Department of Pathology, Johns Hopkins University School of Medicine, Baltimore, Maryland [5]Departments of Pathology and Translational Molecular Pathology, University of Texas MD Anderson Cancer Center, Houston, Texas [6]Department of Biomedicine, Centre for Cancer Biomarkers, Norwegian Centre of Excellence, University of Bergen, Bergen, Norway [7]Department of Pharmacology, University of Texas Southwestern Medical Center, Dallas, Texas, USA

Abstract

Activation of the receptor tyrosine kinase Axl is associated with poor outcomes in pancreatic cancer (PDA), where it coordinately mediates immune evasion and drug resistance. Here we demonstrate that the selective Axl kinase inhibitor BGB324 targets the tumor-immune interface to blunt the aggressive traits of PDA cells *in vitro* and enhance gemcitibine efficacy *in vivo*. Axl signaling stimulates the TBK1-NFκB pathway and innate immune suppression in the tumor microenvironment. In tumor cells, BGB324 treatment drove epithelial differentiation, expression of nucleoside transporters affecting gemcitabine response and an immune stimulatory microenvironment. Our results establish a preclinical mechanistic rationale for the clinical development of Axl inhibitors to improve the treatment of PDA patients.

Keywords

BGB324; Axl; Gas6; metastasis; pancreatic cancer

INTRODUCTION

Pancreatic ductal adenocarcinoma (PDA) is an aggressive human malignancy with a 5-year survival rate of ~7% and a median survival of approximately 6 months (1). Despite all available treatment options, patient survival has not significantly changed in 20 years. PDA

*Corresponding author: Rolf A. Brekken, PhD, Hamon Center for Therapeutic Oncology Research, UT Southwestern, 6000 Harry Hines Blvd., Dallas, TX 75390-8593, Tel: 214.648.5151; Fax: 214.648.4940, rolf.brekken@utsouthwestern.edu.
†Equal contribution
‡Current address: Human Therapeutics Division, Intrexon Corp., Germantown, Maryland

frequently recurs with metastatic disease in the liver, lung, and/or peritoneal cavity. Currently, gemcitabine alone or in combination with nab-paclitaxel is the standard of care but these regimes provide only modest therapeutic benefit (2). New therapeutic agents that target tumor cell pathways associated with chemoresistance are needed as pancreatic cancer is expected to become the second-leading cause of cancer-related death in the United States by 2030 (1).

A prominent chemoresistance strategy exploited by tumor cells is epithelial plasticity (3). Tumor cells activate cellular plasticity related to epithelial-to-mesenchymal transition (EMT) in response to inflammation, nutrient/oxygen deprivation and cellular stress. EMT provides access to a range of tumor cell phenotypes including changes in gene expression, morphological alterations and resistance to cytotoxic therapy (4). Epithelial plasticity is associated with tumor cell evasion of immune surveillance (5). The immune system is a key component of chemotherapy responses and many chemotherapeutic agents, including gemcitabine, directly affect the immune landscape of tumors (6). For example, gemcitabine has been reported to decrease circulating myeloid-derived suppressor cells and support an immune stimulatory phenotype in tumor macrophages (6). Hence, chemotherapeutic resistance mechanisms comprise both tumor intrinsic and immune suppressive features. Identification of key signaling pathways that drive epithelial plasticity and reduce immune surveillance could reveal new therapeutic targets that augment chemotherapeutic efficacy.

Receptor tyrosine kinases (RTKs) are a class of therapeutic targets that have led to successful treatments for a variety of cancers. Axl is a member of the TAM (Tyro3, Axl, MerTK) subfamily of RTKs that participates in various cellular processes, including cell survival, proliferation and migration, epithelial plasticity and the regulation of innate immune responses (7). Axl is expressed by a broad range of malignant tumor types where its activity is associated with a more aggressive, drug resistant, and mesenchymal phenotype (8). Growth arrest specific factor 6 (Gas6), a member of the vitamin K-dependent protein family, is the ligand for Axl (9). However, there is evidence that Axl can be activated in alternative ligand-independent manners (10). The Gas6-Axl pathway is estimated to be active in 70% of human PDA (11), where it is associated with an adverse clinical prognosis (12). Further, preclinical *in vivo* studies have demonstrated that silencing Axl gene expression in PDA tumor cells blocks tumor cell invasion and enhances animal survival (13). Additionally, we recently demonstrated that pharmacologic inhibition of Gas6 activity impaired pancreatic tumor growth and metastatic spread in an Axl-dependent manner (14). Axl, which is also expressed by innate immune cells, including natural killer (NK) cells (15) and tumor-associated macrophages (16), has been implicated in immune suppression (17). Thus, systemic Axl inhibition may enhance the efficacy of cancer therapy through multiple mechanisms.

BGB324 is a first-in-class, highly selective, Axl tyrosine kinase inhibitor, currently in phase II clinical trials for multiple cancers. Several reports demonstrate that BGB324 displays Axl-specific anti-tumor and anti-metastatic activity in murine models of breast and lung cancer (18). In this study, we show that BGB324 combined with gemcitabine was efficacious in robust models of PDA, including patient-derived xenografts (PDX), and in syngenic and genetic models of PDA. BGB324 inhibited Axl in human and murine pancreatic tumor cell

lines *in vitro* where it reduced the growth, motility, and migration of PDA cells. Moreover, Axl inhibition reduced the activity of the innate immune kinase and Ras-effector, tank-binding kinase 1 (TBK1), altered the immune cytokine landscape, and reduced tumor-associated macrophage levels in immune competent models of PDA. These novel findings provide strong evidence that BGB324 may be a promising therapeutic option for the treatment of PDA.

MATERIALS AND METHODS

Study Design

The overall objective of this study was to determine whether Axl inhibition with the small-molecule BGB324 could sensitize well-established mouse models of PDA (*KIC*, Pan02 and PDX) to chemotherapy and determine if Axl inhibition altered the immune landscape of PDA. Western blot, immunocytochemistry, cell migration, colony formation and MTS assay were performed to assess the signaling and biological effects of BGB324 in mouse and human PDA cell lines. *In vitro* analyses were performed three independent times. Western blot, immunofluorescence and immunohistochemistry studies were performed to assess the effect of BGB324 on tumor cells and immune cells in tissues from PDA mouse models. Analysis of tumor tissue was performed at least two independent times, with some markers or analyses performed by different people multiple times. ELISA-based Milliplex were conducted to assess the effect of BGB324 on chemokine and cytokine expression in tissues from PDA mouse models. For PDA mouse models, mice were randomized to each experimental arm and treatment group. Mice were weighed twice weekly and sacrificed when they were moribund or had >20% weight loss. For each experiment, sample size is provided in the figure legend.

Cell Lines

Human pancreatic cancer cell lines (AsPC-1, Panc-1, Capan-1, and Mia PaCa-2) were obtained from ATCC (Manassas, Virginia), and a murine cell line Pan02 was obtained from the Developmental Therapeutics Program at the National Cancer Institute at Frederick, Maryland. KPC-M09 cells were derived from *KPC* PDA mice as described in the supplementary methods. All cell lines were cultured in DMEM (Invitrogen) or RPMI (Invitrogen) containing 10% FBS and maintained in a humidified atmosphere with 5% CO_2 at 37°C. The human cell lines were DNA fingerprinted for provenance using the Power-Plex 1.2 kit (Promega) and confirmed to be the same as the DNA fingerprint library maintained by ATCC. All cell lines were confirmed to be free of mycoplasma (e-Myco kit, Boca Scientific) before use.

Animal Studies

Genetically engineered mouse model: $Kras^{LSL\text{-}G12D}$; $Cdkn2a^{fl/fl}$; $Ptf1a^{Cre/+}$ (*KIC*) mice were generated as previously described (19). At 7 weeks of age (day 49 of life), male and female mice were randomized to receive vehicle (0.5% [w/w] hydroxypropyl methylcellulose/0.1% [w/w] Tween 80 in water, control, PO BID), BGB324 (50 mg/kg PO BID), gemcitabine (25 mg/kg IP twice/week), or gemcitabine + BGB324. Mice were

weighed twice weekly and sacrificed when they were moribund or had >20% weight loss. Tissues were fixed in 10% formalin or snap-frozen in liquid nitrogen for further studies.

Syngenic model: Female 4- to 6-week-old *C57BL/6* mice were obtained from an on-campus supplier. Pan02 cells (5×10^5) were injected orthotopically as described (19). Tumor implantation was confirmed by sonography. Seventeen days after tumor cell implantation, mice were randomized to receive therapy. Treatment groups were the same as described above; however, BGB324 was dosed at 100 mg/kg BID. Mice were weighed twice weekly and sacrificed when they were moribund or had >20% weight loss. Tissues were fixed in 10% formalin or snap-frozen in liquid nitrogen for further studies.

PDX models: Three human pancreatic cancer patient-derived xenografts (Panc 163, Panc 281 and Panc 265) from the 'PanXenoBank' established at Johns Hopkins University (Baltimore, MD) were used for study. Panc 163 and Panc 281 tumors were subcutaneously implanted and Panc 265 tumors were orthotopically implanted in 6-week old male *nu/nu* athymic mice (Harlan). Subcutaneous tumor volumes were measured twice weekly by digital caliper measurements. Orthotopic tumor establishment in the pancreas was assessed initially by transabdominal palpations and confirmed by an ultrasound scan (Vevo 660 VisualSonics, Toronto, ON, Canada). Mice with tumor volume of 150–200 mm^3 were selected and randomly allocated into treatment arms mentioned above with BGB324 at 50 mg/kg BID. Mice were sacrificed after 6 or 4 weeks of therapy in the subcutaneous or orthotopic models, respectively. Upon autopsy, mice in the orthotopic experiment were screened visually for metastatic lesions in the spleen, small intestine, kidneys, liver, lungs and lymph nodes using a 2.5X lens. Tumor volumes were calculated using the following formula: $V = (a \times b^2)/2$, where "a" is the largest dimension and "b" the smallest.

Histology and Tissue Analysis

Formalin-fixed tissues were embedded in paraffin and cut in 5 μm sections. Sections were evaluated by H&E and immunohistochemical analysis using antibodies specific for vimentin (Cell Signaling, 5741), endomucin (Santa Cruz, 65495), E-cadherin (Cell Signaling, 3195), phospho-histone H3 (Millipore, 06-570), cleaved caspase-3 (Cell Signaling, 9664), equilibrative nucleoside transporter 1 (ENT1, Abcam, AB135756), F4/80 (Novus, NBP2-12506), Arginase 1 (Arg1, Santa Cruz, sc-18351). Negative controls included omission of primary antibody. Immunofluorescence evaluation was conducted as described (19). Fluorescent images were captured with a Photometrics CoolSNAP HQ camera using NIS Elements AR 2.3 Software (Nikon). Color images were obtained with a Nikon Eclipse E600 microscope using a Niko Digital Dx1200me camera and ACT1 software (Universal Imaging Corporation). Pictures were analyzed using NIS Elements (Nikon).

Statistical Analysis

Data are reported as means ± SD. Statistical analyses of *KIC* and Pan02 mouse model survival data were performed using analysis of variance (ANOVA) with Mantel-Cox test of significance difference using GraphPad Prism software (GraphPad Prism version 4.00 for Windows; GraphPad Software; www.graphpad.com). Statistical analysis of

immunofluorescence and immunohistorchemistry was performed by *t* test using GraphPad Prism. For all analyses, $P < 0.05$ was considered significant.

Additional methods are described in the supplementary material.

Study Approval

All animals were housed in a pathogen-free facility with 24-hour access to food and water. Experiments were approved by, and conducted in accordance with, the Institutional Animal Care and Use Committee at the University of Texas Southwestern Medical Center (Dallas, Texas) or Johns Hopkins School of Medicine (Baltimore, Maryland), which are compliant with the guidelines proposed by the NIH Guide for the Care and Use of Laboratory Animals.

RESULTS

Resistance to chemotherapy impedes durable clinical responses in patients diagnosed with PDA. We considered that a selective anti-Axl therapy might increase the efficacy of the deoxcytidine analog, gemcitabine. We employed BGB324, a potent, clinical stage Axl-selective small molecule inhibitor with a 15-fold greater inhibitory efficacy for Axl when compared to 133 tyrosine and serine/threonine kinases. BGB324 treatment inhibited basal phosphorylated Axl (pAxl) levels (Figs. 1A–1D) as well as downstream Axl signaling in AsPC-1 cells in a concentration-dependent manner (Fig. 1A), reduced Gas6-stimulated pAxl levels and downstream Axl signaling in Panc-1 cells (Figs 1B), and inhibited antibody-mediated activation of Axl (20) in a murine PDA cell line (Pan02) (Fig. 1C). BGB324 also reduced cell migration (Fig. 1E) and colony formation (Fig. 1F) in established human and primary mouse PDA cell lines at clinically achievable doses (21).

To further investigate the anti-proliferative effect of Axl inhibition, we examined the effect of BGB324 in 6 human and 3 mouse PDA cell lines *in vitro* by MTS assay (Fig. 1G). BGB324 reduced cell number in a dose-dependent manner with IC_{50} values ranging from 1–4.0 μM. Axl has been implicated in chemotherapy resistance and Axl inhibition has been shown to enhance the efficacy of various chemotherapeutic agents across a spectrum of malignancies (10,22). In light of these findings, we tested whether BGB324 at 0.5 μM, a clinically achievable dose, enhanced the response of Pan02, ASPC-1, and MiaPaca2 cells to gemcitabine. Notably, BGB324 reduced the *in vitro* IC_{50} value of gemcitabine a modest 3-fold in all cell lines (Fig. 1H).

In contrast to the modest sensitization of gemcitabine by BGB324 *in vitro*, we observed a dramatic effect of this therapeutic combination on overall survival *in vivo* in mice bearing large advanced PDA tumors, reflective of the typical clinical presentation of PDA. *KIC* ($Kras^{LSL\text{-}G12D}$; $Cdkn2a^{lox/lox}$; $Ptf1a^{Cre/+}$) mice were treated with vehicle ($n = 30$), BGB324 (50 mg/kg; $n = 10$), gemcitabine (25 mg/kg; $n = 15$), or the combination of BGB324 + gemcitabine ($n = 18$) until animals were moribund. Therapy was initiated at 7 weeks of age (d49) when mice displayed advanced disease (Supplementary Fig. 1). Mice that received vehicle had a median survival of 61.5 days, while treatment with BGB324 or gemcitabine only modestly extended the median survival to 65 and 69 days, respectively (*P* value of 0.03 and <0.001 vs. controls). However, combination therapy significantly improved survival to a

median of 83.5 days (*P* value < 0.0001 vs. control; *P* value < 0.05 vs. gemcitabine alone) (Fig. 2A).

Given our *in vitro* data demonstrating the high expression of Axl in the Pan02 cell line (14), we evaluated the effect of gemcitabine and BGB324 in Pan02 tumors *in vivo. C57BL/6* mice were injected orthotopically with Pan02 cells and treated as indicated above with late-stage therapy initiated at day 17 post tumor cell injection (TCI), 6 days prior to initial morbidity in the control group. Similar to the *KIC* model (Fig. 2A), the combination of BGB324 and gemcitabine significantly increased survival (Fig. 2B). All vehicle and single-agent (BGB324 or gemcitabine) treated animals succumbed to disease progression by 44 days post TCI; however, 6/9 animals treated with the combination remained alive 48 days post TCI (*P* < 0.0001 vs. controls or gemcitabine) (Fig. 2B).

We next conducted transcriptome analysis in PDX models of PDA (Fig. 2C). Panc265, a human PDX resistant to gemcitabine therapy, and highly aggressive in the orthotopic setting (23,24), had the highest expression of Axl (Supplementary Fig. 2). This is consistent with prior studies demonstrating that Axl contributes to chemotherapy resistance (25). To determine the *in vivo* efficacy of Axl inhibition with BGB324, we treated established (200 mm^3) subcutaneous PDX tumors (Panc163 and 281, Supplementary Fig. 2) with vehicle, BGB324, gemcitabine, or the combination. Xenograft growth was significantly attenuated by combination therapy (Fig. 2D). In an orthotopic setting, primary Panc265 tumor growth was also effectively controlled by combination therapy. Notably, BGB324 alone or in combination with gemcitabine was remarkably effective in preventing the development of metastasis to different organs and lymph nodes when compared to gemcitabine alone (Fig. 2E). In fact, there was a significant difference in metastasis rate between the BGB324 and control groups (metastases rate: 8.33% vs. 78.57%, p = 0.001; Fisher's exact test) and between the BGB324 and gemcitabine groups (metastases rate: 8.33% vs. 58.33%, p = 0.001; Fisher's exact test). However, there was no significant difference between the BGB324 and combination groups (metastases rate: 8.33% vs. 10.71%, p = 0.999). We also compared the rates of metastasis between different treatment groups, adjusting for different organs using the multivariable exact logistic regression method. It shows a significant difference between BGB324 and control groups (adjusted p <0.0001), and between BGB324 and gemcitabine groups (adjusted p <0.0001), but no significant difference between BGB324 and combination groups (adjusted p =0.999).

We found that Axl inhibition in combination with gemcitabine increased tumor cell apoptosis (increased cleaved-caspase3), decreased tumor cell proliferation (decreased p-histone H3), and reduced microvessel density (decreased endomucin) in genetic *KIC* and syngenic Pan02 tumors (Fig. 3A and Supplementary Fig. 3). The effect of BGB324 treatment on *KIC* tumors was consistent with the effects on Axl signaling *in vitro*, as BGB324 treatment substantially suppressed Akt activation in tumors (Fig. 3B). Combination therapy also reduced activation of S6, Erk1/2, and p38 in *KIC* tumors, further supporting the effect of Axl inhibition on signaling pathways associated with tumor cell survival and proliferation (Fig. 3B).

Axl has been shown to maintain epithelial plasticity (14,26), which contributes to metastasis and chemotherapy resistance (27). Thus, we assessed tumor sections in this study for epithelial (E-cadherin) and mesenchymal (vimentin) markers by immunofluorescence. Consistent with our prior studies (14), we found that untreated *KIC* and Pan02 tumors displayed a robust mesenchymal-like phenotype; however, treatment with BGB324 promoted a differentiated epithelial tumor cell phenotype (Fig. 3A and Supplementary Fig. 3). Notably, this shift was not observed in the tissue of gemcitabine-treated animals. Inhibition or prevention of epithelial plasticity has been shown to sensitize PDA GEMM tumors to gemcitabine chemotherapy through the increased expression of equilibrative nucleoside transporter (ENT1) (28). Similarly, we found inhibition of epithelial plasticity with BGB324 in combination with gemcitabine stimulated expression of ENT1 in *KIC* tumor tissues (Fig. 3C). Hence BGB324 effectively targets a central drug resistance mechanism in PDA.

Axl is expressed by various classes of innate immune cells, such as NK cells and tumor-associated macrophages, and participates in efferocytosis, an immune suppressive mechanism (17). Thus, Axl has been implicated as a potential driver of immune suppression in the tumor microenvironment (15,29,30). To determine if Axl inhibition altered the innate immune landscape of PDA, we first assessed the levels of immune-related cytokines and chemokines after Axl inhibition in the *KIC* GEMM of PDA (Supplementary Table 1). We found that BGB324 suppressed the levels of CCL11, IL-7, IL-1β, and IL-6 (Fig. 4A), which can activate MDSCs and strongly inhibit anti-tumor reactivity of dendritic cells, macrophages, T cells, and NK cells (31). The TBK1/NF-κB pathway is a key signaling pathway in innate immune cells and tumor cells that can stimulate cytokine expression and decrease dendritic cell activity (32). Therefore, we assessed the level of TBK1 signaling in *KIC* tumors treated with BGB324. BGB324 potently inhibited the activation of TBK1 and its downstream targets p65 and IRF3 in *KIC* tumor lysates (Fig. 4B and Supplementary Fig. 4). We further validated that BGB324 suppressed TBK1/NF-κB activation in AsPC-1 and Panc-1 cells (Figs. 4C and 4D). These data indicate that the inhibition of Axl can alter the composition of chemokines and cytokines in the PDA tumor environment potentially through the blockade of TBK1/NF-κB signaling.

We also evaluated the infiltration of macrophages into *KIC* tumors treated with BGB324. BGB324 therapy in *KIC* mice resulted in reduced tumor associated F4/80^{+} macrophages (Fig. 4E and Supplementary Fig. 5). Further, expression of Arginase-1 was also reduced in *KIC* tumors after treatment with BGB324 alone or in combination with gemcitabine (Fig. 4E). *In vitro* studies with IL-4-stimulated primary mouse bone marrow-derived macrophages confirmed that BGB324 treatment can decrease the expression of Arginase-1 in M2-skewed macrophages (Supplementary Fig. 6). We also analyzed the myeloid cell compartment of subcutaneous KPC-M09 tumors after 2 weeks of monotherapy with BGB324 (Fig. 4F and Supplementary Fig. 7). KPC-M09 is a cell line derived from a *KPC* (*Kras*$^{LSL\text{-}G12D}$; *Trp53*$^{LSL\text{-}R172}$; *Ptf1a*$^{Cre/+}$) primary tumor. Therapy with BGB324 for 2 weeks had no effect on primary subcutaneous tumor growth (data not shown) or CD11b^{+} cell numbers associated with the tumor (Supplementary Fig. 7). However, BGB324 did reduce monocytic MDSC (M-MDSC), PDL1^{+} M-MDSC, tumor associated macrophages (TAMs) and Arg1^{+} TAMs consistent with the results in *KIC* and Pan02 tumors.

DISCUSSION

Axl activity has been linked to the progression of PDA (11–13). We demonstrated that BGB324 effectively inhibits Axl activation and Axl-induced signaling in PDA cells *in vitro* and *in vivo*. Axl inhibition with BGB324 reduced colony formation and migration of PDA cells and resulted in modest improvements in the efficacy of gemcitabine *in vitro*. However, the combination of BGB324 and gemcitabine provided striking efficacy in multiple murine models of PDA. Axl inhibition *in vivo* was associated with an increase of epithelial differentiated tumor cells and an altered immune landscape. These phenotypic changes in the tumor microenvironment after Axl inhibition are consistent with known functions of Axl, namely epithelial plasticity and immune suppression. Our studies support that pharmacologic inhibition of Axl is achievable with BGB324 and provides substantial benefit in combination with standard therapy in preclinical models of PDA.

The combination of BGB324 and gemcitabine significantly prolonged survival in murine models of advanced PDA and reduced tumor burden in endpoint assays using three different PDX models. In each survival experiment, control-treated animals succumbed to disease burden only days after therapy began. Further, gemcitabine therapy offered minimal to no therapeutic advantage; in contrast, combination therapy significantly prolonged mouse survival by weeks. Additionally, metastatic burden was reduced in an aggressive orthotopic PDX that is poorly responsive to gemcitabine. These studies are highly supportive of Axl activity in tumor and stromal cells contributing to PDA progression. However, additional studies are required regarding the signaling consequences of Axl inhibition. Our prior investigation demonstrated that Gas6-induced Axl signaling on tumor cells is critical for the metastatic spread of Axl-expressing PDA tumor cells (14); yet non-ligand-induced Axl activation has been observed in multiple cell and tumor systems (33). It is anticipated that the inhibition of Axl with a small molecular weight compound such as BGB324 will disrupt ligand-independent and -dependent Axl activation but this has not been investigated rigorously. Further, the signaling mediators directly downstream of Axl are unclear. Identification of the signal cascade induced by Axl under different conditions will likely require the elucidation of the critical tyrosine phosphorylation events on Axl, which are also unclear at the present time. Thus, while we showed that Axl inhibition with BGB324 reduces the phosphorylation of Akt and TBK1 and subsequent downstream kinases, the connection of Axl to Akt and TBK1 is not well-defined. Additionally, the connection of Axl to downstream signal mediators is likely to depend on the cell type and oncogenotype of that cell.

Induction of epithelial plasticity is associated with tumor progression (34), chemoresistance (35–37), and immune suppression (7,17,29,30,38). Our data showing that BGB324 can reduce tumor progression, increase chemosensitivity, and alter the immune landscape are consistent with observations regarding Axl inhibition by other groups using multiple tumor model systems (18,22,39,40). For example, Ben-Batalla et al. (41) have recently shown that BGB324 can inhibit the growth of chronic myeloid leukemia cells that are resistant to BCR-ABL targeted therapies. Del Pozzo Martin et al. (42) and Gjerdrum et al. (26) demonstrated that Axl was required for EMT-mediated breast cancer metastasis. Kimani et al. (34) showed that inhibition of Gas6-induced TAM activation with novel inhibitors reduces

tumorigenicity. Kasikara et al. (29) found that TAM receptors promote Akt-dependent chemoresistance and PD-L1 expression via ligand-dependent sensing of externalized phosphatidylserine. Finally, a recent study by Kariolis et al. (43) employed a decoy Axl receptor strategy and found potent inhibition of the progression of 4T1, OVCAR8, and SKOV3 tumors. In that study, they compared the efficacy of their Axl receptor decoy to BGB324 in the treatment of 4T1-bearing animals. Unfortunately, they dosed animals at 12.5 mg/kg BID, a dose that is ~4x lower than required for efficacy; thus the results are not an accurate representation of the efficacy of BGB324.

Our data highlight that Axl can activate TBK1, a previously unappreciated aspect of Axl signaling. TBK1 is an innate immune kinase and Ras effector that is downstream of Ral G protein activation (44). TBK1 has been linked to the survival of mutant Kras-expressing cells (45) and can directly activate Akt (46). It is plausible that Axl stimulation of Ras results in Ral-mediated activation of TBK1 in PDA cells. TBK1 is also a critical mediator of innate immune signals that result in interferon type I production and expression of interferon-regulated genes (47). Further, TBK1 has recently been shown to limit the maturation of dendritic cells. Xiao et al. (32) found that the conditional deletion of TBK1 from dendritic cells resulted in T cell activation, the promotion of autoimmunity, and enhanced T cell-mediated tumor immunity. We examined the phosphorylation of TBK1 given the changes in cytokines observed in *KIC* and Pan02 tumors after Axl inhibition, as TBK1 activity has been linked to cytokine expression previously (48,49). Our results suggest that TBK1 activity downstream of Axl is important for tumor cell survival and potentially tumor cell phenotype. Additionally, our studies suggest that the inhibition of Axl may indirectly limit TBK1 activity in immune cells, which might have significant implications regarding the combination of Axl inhibition and immune checkpoint blockade. This is supported in part by our observations that Axl inhibition with BGB324 reduced the expression of Arginase-1, a key player in immunosuppression (50,51), in tumors and isolated macrophages. However, given that the connection between Axl and TBK1 is yet to be defined molecularly, the contribution of TBK1 inhibition to the changes in cytokines and tumor associated myeloid cells after Axl inhibition requires additional validation.

Resistance to chemotherapy remains the major challenge in the treatment of pancreatic cancer. Tumor-intrinsic and suppressive immune mechanisms contribute to chemotherapy failure (52). Our study offers preclinical validation that combination therapy with an Axl inhibitor targets key resistance mechanisms and thus may offer a therapeutic strategy to improve patient responses to gemcitabine, the standard regimen for the treatment of PDA. BGB324 is currently in phase II clinical trials as a single agent and in combination with targeted-, chemo-, and immunotherapy (AML, NCT02488408; NSCLC, NCT02424617, NCT02922777; melanoma, NCT02872259). Our study introduces a rationale for a new therapeutic approach to enhance the efficacy of standard therapy in PDA.

Supplementary Material

Refer to Web version on PubMed Central for supplementary material.

Acknowledgments

Financial support: The work was supported by NIH grants R21 CA173487, R01 CA192381, and U54 CA210181 (PI: M. Ferrari) to R.A. Brekken; T32 CA136515 (PI: J. Schiller) to K.F. Ludwig; T32 GM007062 (PI: D. Mangelsdorf) and F31 CA19603301 to N.B. Sorrelle; T32 CA124334 (PI: J. Shay) to V.H. Cruz; T32 GM008203 (PI: M. Cobb) to M. Topalovski; a sponsored research agreement from BerGenBio to R.A. Brekken; the Effie Marie Cain Scholarship in Angiogenesis Research to R.A. Brekken; and Helse Vest (project No. 911559) to J.B. Lorens. The funders had no role in study design, data collection and analysis, decision to publish, or preparation of the manuscript.

The authors thank D. Primm and Drs. A. Schroit, T. Wilkie, and J. Minna for critical comments on the text and the members of the Brekken and Lorens laboratories for advice and helpful discussion. We also thank Dr. Hong Zhu for statistical evaluation of the metastatic table associated with Figure 2.

References

1. Rahib L, Smith BD, Aizenberg R, Rosenzweig AB, Fleshman JM, Matrisian LM. Projecting cancer incidence and deaths to 2030: the unexpected burden of thyroid, liver, and pancreas cancers in the United States. Cancer Res. 2014; 74(11):2913–21. [PubMed: 24840647]
2. Tempero MA, Malafa MP, Behrman SW, Benson AB 3rd, Casper ES, Chiorean EG, et al. Pancreatic adenocarcinoma, version 2. 2014: featured updates to the NCCN guidelines. J Natl Compr Canc Netw. 2014; 12(8):1083–93. [PubMed: 25099441]
3. Voon DC, Huang RY, Jackson RA, Thiery JP. The EMT spectrum and therapeutic opportunities. Mol Oncol. 2017; 11(7):878–91. [PubMed: 28544151]
4. Wang Z, Li Y, Ahmad A, Banerjee S, Azmi AS, Kong D, et al. Pancreatic cancer: understanding and overcoming chemoresistance. Nat Rev Gastroenterol Hepatol. 2011; 8(1):27–33. [PubMed: 21102532]
5. Dongre A, Rashidian M, Reinhardt F, Bagnato A, Keckesova Z, Ploegh HL, et al. Epithelial-to-Mesenchymal Transition Contributes to Immunosuppression in Breast Carcinomas. Cancer Res. 2017; 77(15):3982–89. [PubMed: 28428275]
6. Galluzzi L, Buque A, Kepp O, Zitvogel L, Kroemer G. Immunological Effects of Conventional Chemotherapy and Targeted Anticancer Agents. Cancer Cell. 2015; 28(6):690–714. [PubMed: 26678337]
7. Lemke G, Rothlin CV. Immunobiology of the TAM receptors. Nat Rev Immunol. 2008; 8(5):327–36. [PubMed: 18421305]
8. Wu F, Li J, Jang C, Wang J, Xiong J. The role of Axl in drug resistance and epithelial-to-mesenchymal transition of non-small cell lung carcinoma. Int J Clin Exp Pathol. 2014; 7(10):6653–61. [PubMed: 25400744]
9. Sasaki T, Knyazev PG, Clout NJ, Cheburkin Y, Gohring W, Ullrich A, et al. Structural basis for Gas6-Axl signalling. EMBO J. 2006; 25(1):80–7. [PubMed: 16362042]
10. Zhang Z, Lee JC, Lin L, Olivas V, Au V, LaFramboise T, et al. Activation of the AXL kinase causes resistance to EGFR-targeted therapy in lung cancer. Nat Genet. 2012; 44(8):852–60. [PubMed: 22751098]
11. Song X, Wang H, Logsdon CD, Rashid A, Fleming JB, Abbruzzese JL, et al. Overexpression of receptor tyrosine kinase Axl promotes tumor cell invasion and survival in pancreatic ductal adenocarcinoma. Cancer. 2011; 117(4):734–43. [PubMed: 20922806]
12. Koorstra JB, Karikari CA, Feldmann G, Bisht S, Rojas PL, Offerhaus GJ, et al. The Axl receptor tyrosine kinase confers an adverse prognostic influence in pancreatic cancer and represents a new therapeutic target. Cancer Biol Ther. 2009; 8(7):618–26. [PubMed: 19252414]
13. Leconet W, Larbouret C, Chardes T, Thomas G, Neiveyans M, Busson M, et al. Preclinical validation of AXL receptor as a target for antibody-based pancreatic cancer immunotherapy. Oncogene. 2014; 33(47):5405–14. Pelegrin and Bruno Robert are inventors on anti-AXL mAb patents related to this work. The others authors declare that they have no competing interests. [PubMed: 24240689]

14. Kirane A, Ludwig KF, Sorrelle N, Haaland G, Sandal T, Ranaweera R, et al. Warfarin Blocks Gas6-Mediated Axl Activation Required for Pancreatic Cancer Epithelial Plasticity and Metastasis. Cancer Res. 2015; 75(18):3699–705. [PubMed: 26206560]
15. Paolino M, Choidas A, Wallner S, Pranjic B, Uribesalgo I, Loeser S, et al. The E3 ligase Cbl-b and TAM receptors regulate cancer metastasis via natural killer cells. Nature. 2014; 507(7493):508–12. [PubMed: 24553136]
16. Ye X, Li Y, Stawicki S, Couto S, Eastham-Anderson J, Kallop D, et al. An anti-Axl monoclonal antibody attenuates xenograft tumor growth and enhances the effect of multiple anticancer therapies. Oncogene. 2010; 29(38):5254–64. [PubMed: 20603615]
17. Akalu YT, Rothlin CV, Ghosh S. TAM receptor tyrosine kinases as emerging targets of innate immune checkpoint blockade for cancer therapy. Immunol Rev. 2017; 276(1):165–77. [PubMed: 28258690]
18. Holland SJ, Pan A, Franci C, Hu Y, Chang B, Li W, et al. R428, a selective small molecule inhibitor of Axl kinase, blocks tumor spread and prolongs survival in models of metastatic breast cancer. Cancer Res. 2010; 70(4):1544–54. [PubMed: 20145120]
19. Ostapoff KT, Cenik BK, Wang M, Ye R, Xu X, Nugent D, et al. Neutralizing murine TGFbetaR2 promotes a differentiated tumor cell phenotype and inhibits pancreatic cancer metastasis. Cancer Res. 2014; 74(18):4996–5007. [PubMed: 25060520]
20. Zagorska A, Traves PG, Lew ED, Dransfield I, Lemke G. Diversification of TAM receptor tyrosine kinase function. Nat Immunol. 2014; 15(10):920–8. [PubMed: 25194421]
21. Hellesøy MGS, Tislevoll BS, Fagerholt OHE, Reikvam H, Loges S, Cortes J, Heuser M, Chromik J, Skavland J, Sulen A, Bruserud Ø, Lorens J, Gausdal G, Micklem D, Gjertsen BT. Single Cell Signaling Pharmacodynamics in a Phase 1b Trial of the Axl Inhibitor BGB324 in Acute Myeloid Leukemia. Blood. 2016; 128:3995.
22. Balaji K, Vijayaraghavan S, Diao L, Tong P, Fan Y, Carey JP, et al. AXL Inhibition Suppresses the DNA Damage Response and Sensitizes Cells to PARP Inhibition in Multiple Cancers. Mol Cancer Res. 2017; 15(1):45–58. [PubMed: 27671334]
23. Rubio-Viqueira B, Jimeno A, Cusatis G, Zhang X, Iacobuzio-Donahue C, Karikari C, et al. An in vivo platform for translational drug development in pancreatic cancer. Clin Cancer Res. 2006; 12(15):4652–61. [PubMed: 16899615]
24. Rajeshkumar NV, Yabuuchi S, Pai SG, Tong Z, Hou S, Bateman S, et al. Superior therapeutic efficacy of nab-paclitaxel over cremophor-based paclitaxel in locally advanced and metastatic models of human pancreatic cancer. Br J Cancer. 2016; 115(4):442–53. [PubMed: 27441498]
25. Martinho O, Zucca LE, Reis RM. AXL as a modulator of sunitinib response in glioblastoma cell lines. Exp Cell Res. 2015; 332(1):1–10. [PubMed: 25637219]
26. Gjerdrum C, Tiron C, Hoiby T, Stefansson I, Haugen H, Sandal T, et al. Axl is an essential epithelial-to-mesenchymal transition-induced regulator of breast cancer metastasis and patient survival. Proc Natl Acad Sci U S A. 2010; 107(3):1124–9. [PubMed: 20080645]
27. Arumugam T, Ramachandran V, Fournier KF, Wang H, Marquis L, Abbruzzese JL, et al. Epithelial to mesenchymal transition contributes to drug resistance in pancreatic cancer. Cancer Res. 2009; 69(14):5820–8. [PubMed: 19584296]
28. Zheng X, Carstens JL, Kim J, Scheible M, Kaye J, Sugimoto H, et al. Epithelial-to-mesenchymal transition is dispensable for metastasis but induces chemoresistance in pancreatic cancer. Nature. 2015; 527(7579):525–30. [PubMed: 26560028]
29. Kasikara C, Kumar S, Kimani S, Tsou WI, Geng K, Davra V, et al. Phosphatidylserine Sensing by TAM Receptors Regulates AKT-Dependent Chemoresistance and PD-L1 Expression. Mol Cancer Res. 2017; 15(6):753–64. [PubMed: 28184013]
30. Aguilera TA, Rafat M, Castellini L, Shehade H, Kariolis MS, Hui AB, et al. Reprogramming the immunological microenvironment through radiation and targeting Axl. Nat Commun. 2016; 7:13898. [PubMed: 28008921]
31. Gabrilovich DI. Myeloid-Derived Suppressor Cells. Cancer Immunol Res. 2017; 5(1):3–8. [PubMed: 28052991]

32. Xiao Y, Zou Q, Xie X, Liu T, Li HS, Jie Z, et al. The kinase TBK1 functions in dendritic cells to regulate T cell homeostasis, autoimmunity, and antitumor immunity. J Exp Med. 2017; 214(5): 1493–507. [PubMed: 28356390]
33. Meyer AS, Miller MA, Gertler FB, Lauffenburger DA. The receptor AXL diversifies EGFR signaling and limits the response to EGFR-targeted inhibitors in triple-negative breast cancer cells. Sci Signal. 2013; 6(287):ra66. [PubMed: 23921085]
34. Kimani SG, Kumar S, Bansal N, Singh K, Kholodovych V, Comollo T, et al. Small molecule inhibitors block Gas6-inducible TAM activation and tumorigenicity. Sci Rep. 2017; 7:43908. [PubMed: 28272423]
35. Davra V, Kimani SG, Calianese D, Birge RB. Ligand Activation of TAM Family Receptors-Implications for Tumor Biology and Therapeutic Response. Cancers (Basel). 2016; 8(12)
36. Rankin EB, Giaccia AJ. The Receptor Tyrosine Kinase AXL in Cancer Progression. Cancers (Basel). 2016; 8(11)
37. Scaltriti M, Elkabets M, Baselga J. Molecular Pathways: AXL, a Membrane Receptor Mediator of Resistance to Therapy. Clin Cancer Res. 2016; 22(6):1313–7. [PubMed: 26763248]
38. Aguilera TA, Giaccia AJ. Molecular Pathways: Oncologic Pathways and Their Role in T-cell Exclusion and Immune Evasion-A New Role for the AXL Receptor Tyrosine Kinase. Clin Cancer Res. 2017; 23(12):2928–33. [PubMed: 28289089]
39. Loges S, Schmidt T, Tjwa M, van Geyte K, Lievens D, Lutgens E, et al. Malignant cells fuel tumor growth by educating infiltrating leukocytes to produce the mitogen Gas6. Blood. 2010; 115(11): 2264–73. [PubMed: 19965679]
40. Wilson C, Ye X, Pham T, Lin E, Chan S, McNamara E, et al. AXL inhibition sensitizes mesenchymal cancer cells to antimitotic drugs. Cancer Res. 2014; 74(20):5878–90. [PubMed: 25125659]
41. Ben-Batalla I, Erdmann R, Jorgensen H, Mitchell R, Ernst T, von Amsberg G, et al. Axl Blockade by BGB324 Inhibits BCR-ABL Tyrosine Kinase Inhibitor-Sensitive and -Resistant Chronic Myeloid Leukemia. Clin Cancer Res. 2017; 23(9):2289–300. [PubMed: 27856601]
42. Del Pozo Martin Y, Park D, Ramachandran A, Ombrato L, Calvo F, Chakravarty P, et al. Mesenchymal Cancer Cell-Stroma Crosstalk Promotes Niche Activation, Epithelial Reversion, and Metastatic Colonization. Cell Rep. 2015; 13(11):2456–69. [PubMed: 26670048]
43. Kariolis MS, Miao YR, Diep A, Nash SE, Olcina MM, Jiang D, et al. Inhibition of the GAS6/AXL pathway augments the efficacy of chemotherapies. J Clin Invest. 2017; 127(1):183–98. the receptor tyrosine kinase AXL" (US8618254 B2), which is related to the work described in this paper, with M.S. Kariolis, Y.R. Miao, D.S. Jones, E.B. Rankin, J.R. Cochran, and A.J. Giaccia named as inventors. A.J. Giaccia and A.C. Koong are cofounders of Ruga Corp., a company that has licensed this patent. [PubMed: 27893463]
44. Cooper JM, Bodemann BO, White MA. The RalGEF/Ral pathway: evaluating an intervention opportunity for Ras cancers. Enzymes. 2013; 34(Pt. B):137–56. [PubMed: 25034103]
45. Chien Y, Kim S, Bumeister R, Loo YM, Kwon SW, Johnson CL, et al. RalB GTPase-mediated activation of the IkappaB family kinase TBK1 couples innate immune signaling to tumor cell survival. Cell. 2006; 127(1):157–70. [PubMed: 17018283]
46. Ou YH, Torres M, Ram R, Formstecher E, Roland C, Cheng T, et al. TBK1 directly engages Akt/PKB survival signaling to support oncogenic transformation. Mol Cell. 2011; 41(4):458–70. [PubMed: 21329883]
47. Hasan M, Yan N. Therapeutic potential of targeting TBK1 in autoimmune diseases and interferonopathies. Pharmacol Res. 2016; 111:336–42. [PubMed: 27353409]
48. Yang S, Imamura Y, Jenkins RW, Canadas I, Kitajima S, Aref A, et al. Autophagy Inhibition Dysregulates TBK1 Signaling and Promotes Pancreatic Inflammation. Cancer Immunol Res. 2016; 4(6):520–30. [PubMed: 27068336]
49. Barbie TU, Alexe G, Aref AR, Li S, Zhu Z, Zhang X, et al. Targeting an IKBKE cytokine network impairs triple-negative breast cancer growth. J Clin Invest. 2014; 124(12):5411–23. [PubMed: 25365225]

50. Ellyard JI, Quah BJ, Simson L, Parish CR. Alternatively activated macrophage possess antitumor cytotoxicity that is induced by IL-4 and mediated by arginase-1. J Immunother. 2010; 33(5):443–52. [PubMed: 20463604]

51. Bhatt S, Qin J, Bennett C, Qian S, Fung JJ, Hamilton TA, et al. All-trans retinoic acid induces arginase-1 and inducible nitric oxide synthase-producing dendritic cells with T cell inhibitory function. J Immunol. 2014; 192(11):5098–108. [PubMed: 24790153]

52. Zitvogel L, Kepp O, Kroemer G. Immune parameters affecting the efficacy of chemotherapeutic regimens. Nat Rev Clin Oncol. 2011; 8(3):151–60. [PubMed: 21364688]

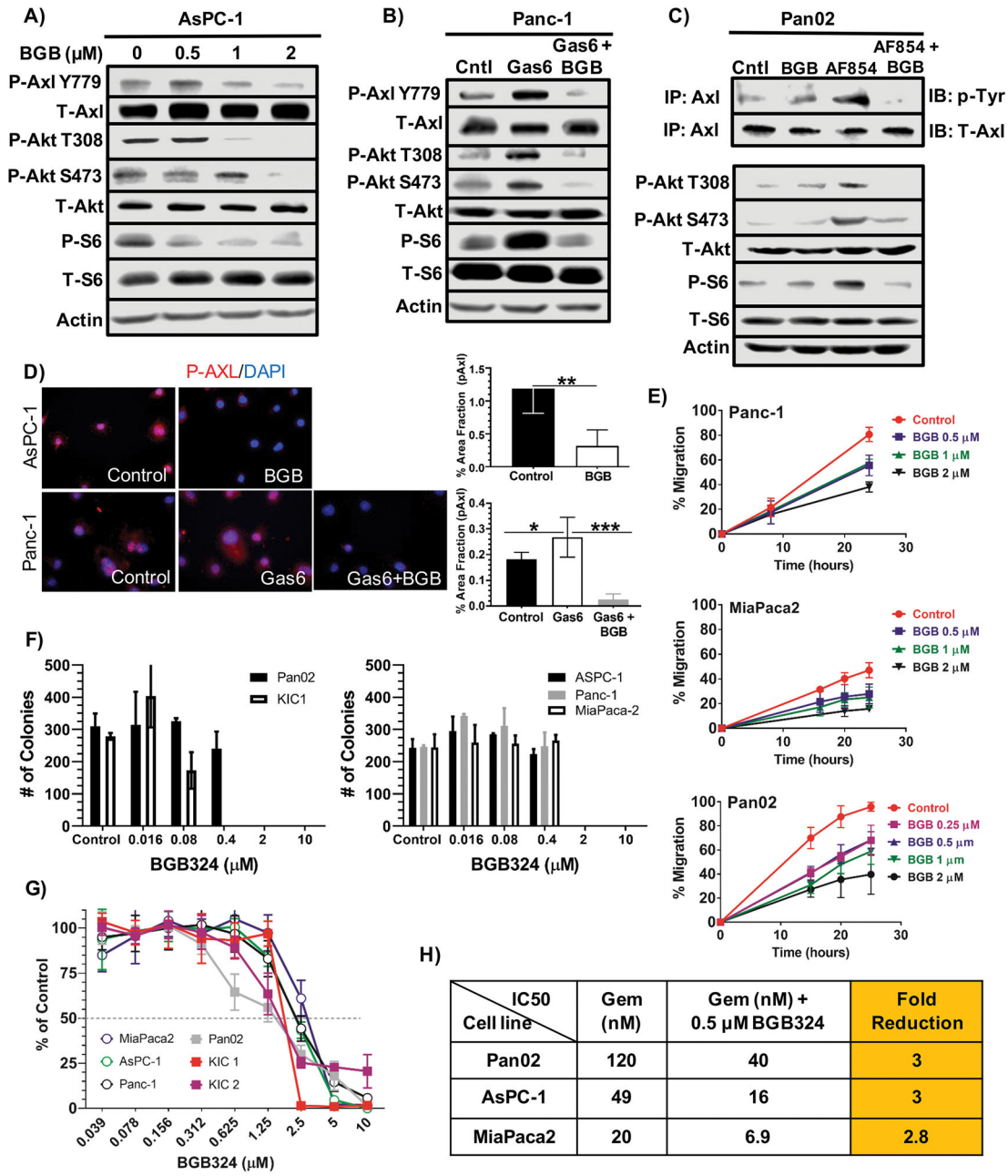

IC50 / Cell line	Gem (nM)	Gem (nM) + 0.5 μM BGB324	Fold Reduction
Pan02	120	40	3
AsPC-1	49	16	3
MiaPaca2	20	6.9	2.8

Figure 1. BGB324 inhibits Axl activity in pancreatic cancer cells *in vitro*

A) AsPC-1 cells were serum starved in 1% FBS in media overnight and subsequently treated with increasing concentrations of BGB324 (BGB) for 30 minutes. Cell lysates were probed by Western blotting for the indicated targets. **B)** Panc-1 cells were serum starved overnight as above and subsequently stimulated with DMSO (0.02%) in media (Cntl), Gas6 (200 ng/ml) or Gas6 + BGB324 (2 μM) for 30 minutes followed by Western blot analysis for the indicated targets. **C)** Pan02 cells were serum starved overnight and subsequently treated with DMSO (0.02%) in media, BGB324 alone (2 μM), AF854 (2.5 nM), an Axl antibody that can stimulate Axl activation (20), or AF854 + BGB324 for 30 minutes. Axl was

immunoprecipitated followed by probing for phospho-tyrosine (p-Tyr) and total Axl (upper two rows). Total cell lysates were also probed for the indicated targets. **D)** Phosphorylated Axl was detected in AsPC-1 and Panc-1 by immunocytochemistry. AsPC-1 cells were serum starved overnight as above (Control) then treated with BGB324 (2 μM) for 30 minutes. Panc-1 cells were serum starved and treated with Gas6 (200 ng/ml) or Gas6 + BGB324 (2 μM). AsPC-1 and Panc-1 cells were fixed permeabilized, stained with anti-phospho-Axl, and subsequently developed by immunofluorescence. Images were analyzed using Elements software; quantification of % area fraction is shown. Data are displayed as mean ± SD and represent 5 images per cell line. $*P < 0.05$; $**P < 0.01$; $***P < 0.005$. **E)** The effect of BGB324 on cell migration was assessed by a "scratch" assay. Monolayers of the indicated cells were wounded with a pipet tip. The cells were incubated in serum-free media +/− BGB324 at the indicated concentrations. Wound closure was monitored at 10, 20, and 30 hours and is reported as % wound closure. **F)** Colony formation for Pan02, *KIC1*, and 3 human PDA cell lines grown in normal growth media +/− BGB324 at the indicated doses for 14 days. Mean + SD colonies/hpf are shown. **G)** Cell growth assays were performed in a 96 well format for 5 days using MTS. Drug sensitivity curves for BGB324 are displayed. **H)** IC_{50} as determined by MTS assay for gemcitabine alone, gemcitabine+BGB324, and fold reduction in presence of BGB324 are displayed.

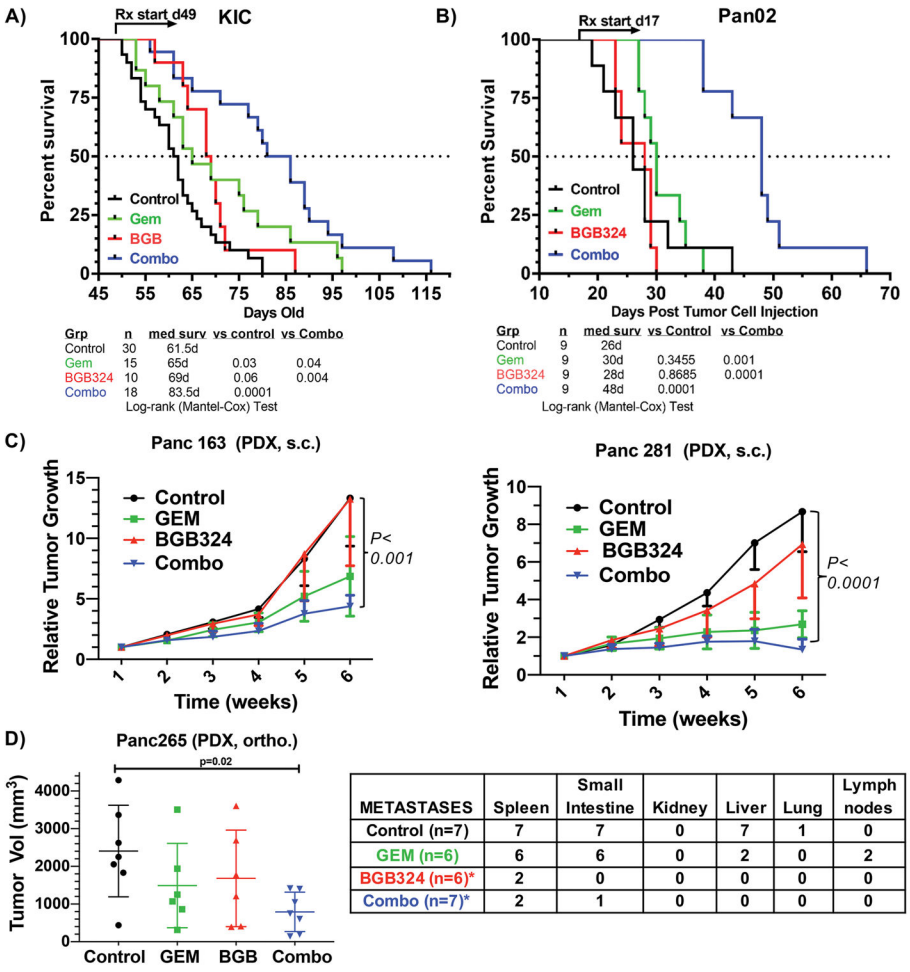

METASTASES	Spleen	Small Intestine	Kidney	Liver	Lung	Lymph nodes
Control (n=7)	7	7	0	7	1	0
GEM (n=6)	6	6	0	2	0	2
BGB324 (n=6)*	2	0	0	0	0	0
Combo (n=7)*	2	1	0	0	0	0

Figure 2. Axl inhibition in mice with advanced PDA improves survival

KIC mice **(A)** and Pan02 tumor-bearing mice **(B)** were enrolled in a survival study and randomized to vehicle (0.5% [w/w] hydroxypropyl methylcellulose/0.1% [w/w] Tween 80 in water, control, PO BID), BGB324 (50 mg/kg PO BID), gemcitabine (25 mg/kg IP twice a week), and gemcitabine + BGB324. Therapy was initiated at day 49 (*KIC*) or day 17 post tumor cell injection (Pan02) and maintained until sacrifice. **C)** *In vivo* assessment of treatment response of subcutaneously (SC) implanted pancreatic PDX. Panc 281 and Panc 163 were implanted SC on the flanks of athymic mice (n = 8–10/group). When tumors were established, mice were treated with vehicle (control, PO BID), BGB324 (50 mg/kg PO BID), gemcitabine (25 mg/kg IP twice a week), or the combination. Effects on tumor growth are shown after 4 weeks of treatment. **D)** Panc 265 was orthotopically implanted into nu/nu athymic mice. After tumor establishment, mice were treated as in (C) (n = 6–7/group). Total gross metastasis was determined by evaluation of liver, diaphragm, GI lymph nodes, and lung at the time of sacrifice. BGB324 alone or in combination with gemcitabine significantly reduced the rate of metastasis (p=*0.001* vs control, Fisher's exact test)

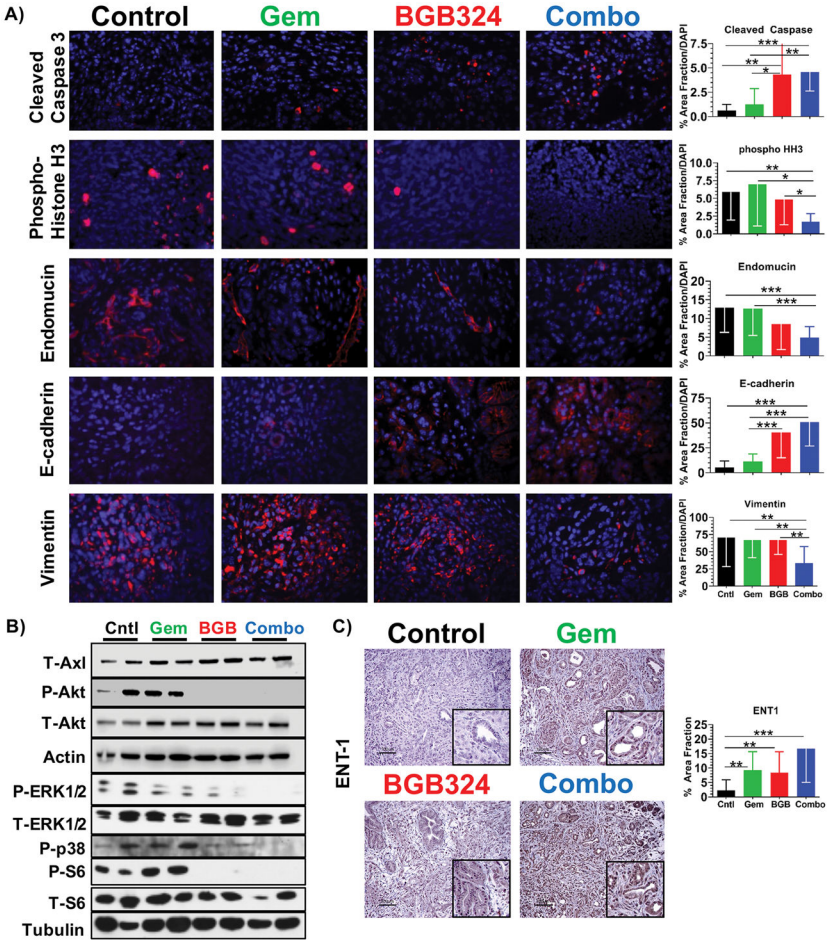

Figure 3. BGB324 in combination with gemcitabine inhibits cell survival and epithelial plasticity

A) Tumor tissue from *KIC* mice treated with BGB324 +/− gemcitabine was evaluated by immunofluorescence for cleaved-caspase 3, phospho-histone-3, endomucin, E-cadherin, and vimentin. Images were analyzed using Elements software; quantification of % area fraction is shown. Data are displayed as mean ± SD and represent 5 images per tumor with 4 animals per group analyzed. *$P < 0.05$; **$P < 0.01$; ***$P < 0.005$; by ANOVA with Tukey's MCT. **B)** Lysates of tumors from *KIC* animals treated with BGB324 +/− gemcitabine were probed for the indicated targets by Western blotting. **C)** Tumor tissue from *KIC* animals treated with BGB324 +/− gemcitabine was evaluated by immunohistochemistry for the expression level of equilibrative nucleoside transporter 1 (ENT1). Quantification of % area fraction is shown. Scale bar, 100 μM.

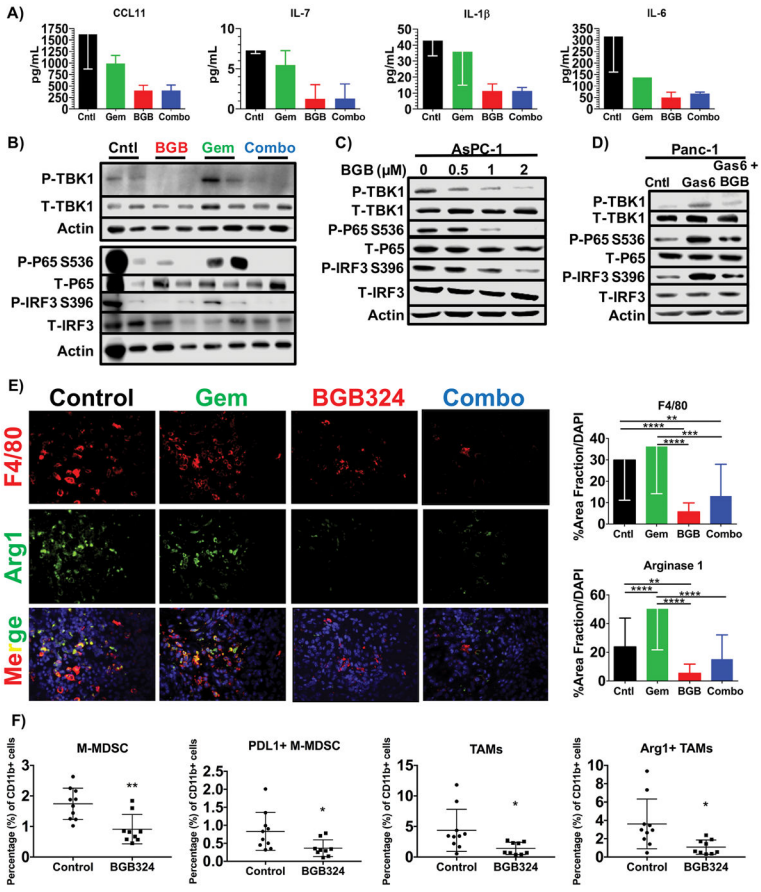

Figure 4. Inhibition of Axl with BGB324 alters the immune landscape of PDA

A) Tumor lysates from *KIC* mice treated with vehicle (Cntl), gemcitabine (Gem), BGB324 (BGB) or the combination (Combo) were analyzed for cytokine context by Milliplex assay. The levels of Ccl11, Il-7, Il-1β, and Il-6 are shown as mean ± SD (n = 2/group). **B)** Tumor lysates from *KIC* animals treated as above were probed for the level of active TBK1 and NF-κB by Western blotting for the indicated targets. **C, D)** The effect of Axl on TBK1 signaling was probed in AsPC-1 (C) and Panc-1 (D) cells by Western blot analysis. AsPC-1 cells were serum starved overnight and subsequently treated with increasing concentrations of BGB324 for 30 minutes. Panc-1 cells were serum starved and subsequently stimulated with control (0.02% DMSO in media), Gas6 (200 ng/ml), or Gas6 + BGB324 (2 μM) for 30 minutes. Tumor cell lysates were probed for phosphorylated TBK1 and downstream targets. **E)** Tumor tissue from *KIC* mice treated with BGB324 +/− gemcitabine were evaluated by immunofluorescence for macrophage (F4/80) and Arginase 1 (Arg1) and counterstained with DAPI. Images were analyzed using Elements software; quantification of % area fraction is shown. Data are displayed as mean ± SD and represent 5 images per tumor with 4 animals per group analyzed. $^{**}P < 0.01$; $^{***}P < 0.005$; $^{****}P < 0.001$; by ANOVA with Tukey's MCT. **F)** Flow cytometry of KPC-M09 subcutaneous tumors treated with vehicle (control) or BGB324 (50 mg/kg, PO, BID) for two weeks as described in the supplementary methods. BGB324 reduced monocytic MDSCs ($CD11b^+$ $Ly6G^-$ $Ly6C^+$), PD-$L1^+$ M-

MDSCs, tumor associated macrophages (TAMs, $CD11b^+$ $Ly6G^-$ $Ly6C^-$ $F4/80^+$ $CD11c^+$ $MHCII^+$) and $Arg1^+$ TAMs. *, $P < 0.05$; **, $P < 0.01$ by t-test.